PRELIMINARY CALIBRATION FOR ACCURATE PREDICTIONS OF MICROSCALE OXYGEN BAROMETRY IN SILICATE GLASSES USING VANADIUM X-RAY ABSORPTION SPECTROSCOPY: A MULTIVARIATE APPROACH. A. Lanzirotti[1], M. Dyar[2], S. Sutton[1], M. Newville[1], E. Head[3], C. Carey[4], M. McCanta[5] and J. Jones[6]. [1]CARS, Univ. of Chicago, Chicago, IL 60439, lanzirotti@uchicago.edu, [2]Planetary Science Institute, 1700 E. Fort Lowell, Tucson, AZ 85719, [3]Dept. of Earth Science, Northeastern Illinois Univ., Chicago, IL 60625, [4]Col. of Information and Computer Sciences, Univ. of Massachusetts, Amherst, MA 01003, [5]Dept. of Earth and Planetary Sciences, Univ. of Tennessee, Knoxville, TN 37996, [6]NASA/JSC, Houston, TX 77058.

Introduction: Accurately constraining the oxygen fugacity (fO_2) of magmatic melts is important for understanding the evolution of planetary interiors. The V valence [1,2] proxy for fO_2 can provide a highly sensitive measure of melt redox in both terrestrial and extraterrestrial magmas. In melts, vanadium can exist as V^{3+}, V^{4+}, and V^{5+}; in some highly reduced extraterrestrial systems V^{2+} may potentially be stable. Because magma fO_2 exerts a primary control on the discrete V valence states that will exist in quenched melts, accurate measurements of the average V valence in magmatic glasses using X-ray absorption near–edge structure (XANES) spectroscopy facilitate development of a precise and accurate V valence oxybarometer.

A previous study [1] developed a calibration curve to relate the intensity of the V XANES pre-edge peak to the effective V valence (V*) in synthetic glasses. That calibration relates oxygen fugacity to V* after correction for the temperature dependence of the various V redox couples. While this calibration is relatively simple to apply, it does not exploit information contained within the entire spectrum, potentially extending into the EXAFS region, which may also be a sensitive measure of the spectroscopic response to changing V valence. For example, the average centroid energy of the V pre-edge peak and the position of the rising absorption edge (E_0) also vary with changes in V*.

Multivariate analysis (MVA) models hold significant promise for the development of calibration models that employ the full XAS spectral range. Applied to Fe XANES in minerals and glasses, such approaches have resulted in dramatic improvements in the accuracy of predicting $Fe^{3+}/\Sigma Fe$ [3]. Two approaches have been applied to the study of XAS data to date: partial least-squares regression, or PLS, and least absolute shrinkage and selection operator, or LASSO. In this study, we use PLS and LASSO to study V in magmatic and volcanic glasses. These MVA models yield significantly more reliable predictions of V* and melt fO_2 than approaches based solely on measuring changes in V pre-edge intensity, with the added benefit of improved precision and accuracy.

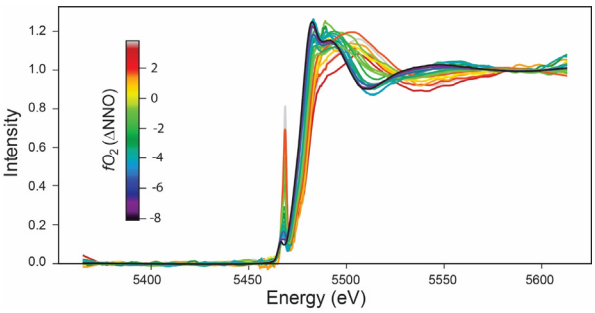

Figure 1. XANES spectra for 20 V-bearing glass standards, color coded as a function of their fO_2 at equilibration (log units relative to the NNO buffer).

Experimental Methods: μXANES data (2 μm beam size) were acquired at the GSECARS 13-ID-E beamline at the Advanced Photon Source. A suite of 20 synthetic glass standards were analyzed, covering both natural basaltic [4] and forsterite-anorthite-diopside (FAD) [5] compositions with V concentrations that range from ~200-300 ppm (basaltic) to 3000 ppm (FAD). The glasses were equilibrated under varying fO_2 conditions, covering a redox range relative to the nickel-nickel oxide (NNO) buffer from NNO-9 to NNO+4 but at similar equilibration temperatures (1320-1350°C).

MVA models were then trained from the μXANES results using the open-source machine learning Python library Scikit-learn [6] and the *Superman* website at http://nemo.cs.umass.edu:54321 [7]. Predictor variables for the MVA models consist of a matrix of intensity values at each of the 331 channels representing incident beam energy for the XANES spectra for each of the 20 samples analyzed. The optimal number of components for the PLS model was 4, while sparsity parameter values of α = 0.01, 0.001, and 0.0001 were tested for LASSO.

Results: Fig. 1 shows the μXANES data that were acquired for the standard glasses, color coded to indicate their fO_2 at equilibration relative to the NNO buffer. As expected, the measured spectra display strong and systematic variations in both the intensity and energy of the pre-edge peak multiplets, E_0, the energy position of the white line, and in the spectral structure immediately following the white line. These conspicuous variations with fO_2 suggest that it ought to be fairly straightforward to develop a predictive model from them.

In Fig. 2, the modeled PLS coefficients are represented as blue dots, with the magnitudes indicated by the distance from zero on the right axis. This PLS model predicts fO_2 with accuracy of ±0.37 log units when the

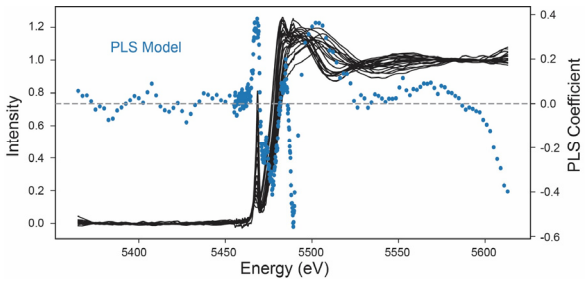

Figure 2. Model results for PLS showing all the spectra (in black) with PLS coefficients superimposed. Positive PLS coefficients are channels that are positively correlated with the channel being predicted and negative ones are the reverse.

full spectral region is employed. The most highly-weighted predictive information for V* and fO_2 occurs both in the pre-edge peak and in the main edge.

Fig. 3 shows the analogous plot for the LASSO models. By varying values of α, we probe which channels are most important in predicting fO_2. For the sparcest model (α = 0.01), there are only four channels (5468.52, 5477.38, 5506.13, and 5477.98 eV), yet those channels predict fO_2 with an accuracy of ±0.56 log units. Decreasing α to 0.001 and 0.0001 yields accuracies of ±0.26 and ±0.05, respectively (using channels in Fig. 3).

Fig. 4 shows the predicted fO_2's relative to NNO

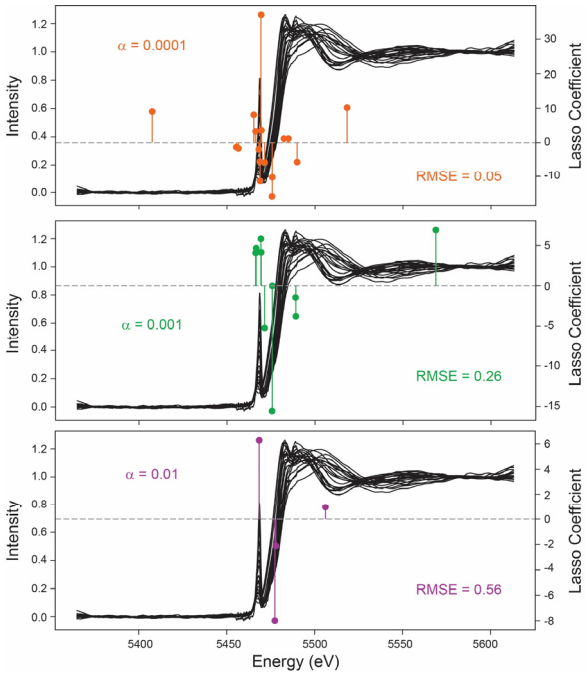

Figure 3. Model results for LASSO with variable values of α; with spectra (black) and coefficients superimposed. The LASSO models are quite sparse (even α = 0.0001 uses just 17 channels), implying that they are highly generalizable.

buffer for all 20 glasses, as calculated by the PLS and LASSO models relative to the values reported for equilibration. Compositional differences between basaltic and FAD glasses appear to have little impact on the predicted oxygen fugacity. In on-going work, we are synthesizing additional V-rich glasses at varying values of fO_2 that should strengthen this calibration further. However, this work suggests that these methods can be used

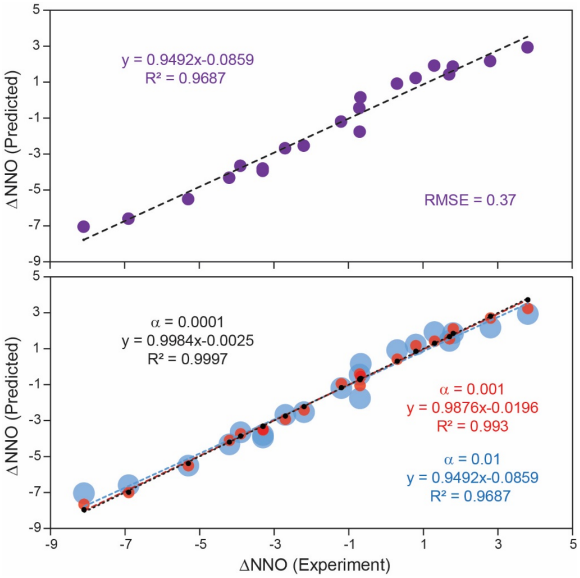

Figure 4. Comparison of the NNO relative fO_2 values predicted by the (top) PLS and (bottom) lasso models to published equilibration values. Symbols scaled to the magnitude of the RMSE values (error bars) for predicted values, α=0.01 (**blue**), α=0.001 (**red**), α=0.0001 (**black**).

across a broad range of glass compositions. They are easily automated, and the sparse models even have the potential of being implemented in mapping fO_2 using a few well-selected energies defined by the MVA model. It is important to appreciate that values of V valence state were not input into these models. Rather, the value for oxygen fugacity was predicted directly. By assuming that NNO and V redox equilibria are parallel, valid if the buffer reaction enthalpy falls within the range of reduction enthalpies for typical redox couples, the model avoids the need to apply large corrections for the temperature dependance in the V valence redox couple.

Acknowledgements: This research was supported by the Remote, In Situ, and Synchrotron Studies for Science and Exploration (RIS^{4}E) node of the NASA SSERVI program and NASA grant NNX16AR18G. GSECARS Sector 13 is supported NSF EAR-1128799 and DOE GeoSciences DE-FG02-94ER14466. We acknowledge support from the Smithsonian Institution NMNH National Rock Collection for the use of NMNH 117393 basalt reference glasses for this study.

References: [1] Sutton S. et al. (2005) *GCA, 69*, 2333–2348. [2] Karner J. et al. (2006) *Am.Min.., 91*, 270–277. [3] Dyar M. et al. (2016) *Am.Min., 101*, 744–747. [4] Cottrell E. et al. (2009) *Chem.Geol., 268*, 167–179. [5] Hanson B. and Jones J. (1998) *Am.Min..*, 83, 669–684. [6] Pedregosa F. et al. (2011) *J. Machine Learning Res., 12*, 2825-2830. [7] Carey C. et al. (2017) *LPS XLVII*, Abstract #1097.